JOURNAL OF SYNCHROTRON RADIATION
ISSN 1600-5775

Hard X-ray-induced damage on carbon–binder matrix for *in situ* synchrotron transmission X-ray microscopy tomography of Li-ion batteries

Cheolwoong Lim,[a] Huixiao Kang,[a] Vincent De Andrade,[b] Francesco De Carlo[b] and Likun Zhu[a]*

[a]Department of Mechanical Engineering, Indiana University–Purdue University Indianapolis, Indianapolis, IN 46202, USA, and [b]Advanced Photon Source, Argonne National Laboratory, Argonne, IL 60439, USA. *Correspondence e-mail: likzhu@iupui.edu

Received 12 December 2016
Accepted 23 February 2017

Edited by J. F. van der Veen

Keywords: radiation damage; Li ion battery; *in situ*; carbon–binder matrix; intermittent dose.

Supporting information: this article has supporting information at journals.iucr.org/s

The electrode of Li-ion batteries is required to be chemically and mechanically stable in the electrolyte environment for *in situ* monitoring by transmission X-ray microscopy (TXM). Evidence has shown that continuous irradiation has an impact on the microstructure and the electrochemical performance of the electrode. To identify the root cause of the radiation damage, a wire-shaped electrode is soaked in an electrolyte in a quartz capillary and monitored using TXM under hard X-ray illumination. The results show that expansion of the carbon–binder matrix by the accumulated X-ray dose is the key factor of radiation damage. For *in situ* TXM tomography, intermittent X-ray exposure during image capturing can be used to avoid the morphology change caused by radiation damage on the carbon–binder matrix.

1. Introduction

Transmission X-ray microscopy (TXM) is an image acquisition technique that captures transmitted monochromatic X-rays through a sample. Recently, the microstructure of porous electrodes of Li-ion batteries (LIBs) has been reconstructed using TXM tomography by collecting a series of TXM images during a 180° rotation of the electrode (Lim *et al.*, 2016). The non-destructive advantage of TXM is that it allows the study of the *in situ* morphology change of high-capacity LIB anode materials, such as Ge (Weker *et al.*, 2014) and Sn (Wang *et al.*, 2014). During *in situ* TXM tomography, the electrode is exposed under a high radiation dose which can cause radiation damage on the electrode. Thus, it is necessary to investigate the radiation-induced damage for *in situ* TXM tomography. Previous studies have shown radiation damage on the LIB electrode (Weker *et al.*, 2014) during *in situ* TXM. However, the root cause of radiation damage is still elusive because all the components of a working LIB cell could be impacted by X-rays and any damage on any component could affect the performance of the cell significantly. Nelson *et al.* (2013) have shown that irradiated sulfur particles were dissolved in electrolyte after 20 s of 6 keV X-ray exposure. Irradiation of an electrode could also affect the carbon–binder matrix because polymers are sensitive to X-ray irradiation (Coffey *et al.*, 2002; Vaselabadi *et al.*, 2016). The objectives of this paper are to investigate the hard X-ray induced damage on the carbon–binder matrix in *in situ* LIB cells and to find ways to avoid the damage.

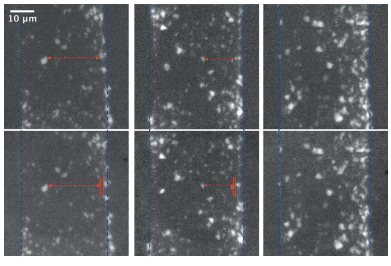

2. Experimental

A wire-shaped electrode was sealed in a 500 µm quartz capillary tube (Hampton Research, Aliso Viejo, CA, USA) which was filled with 1 *M* $LiPF_6$ in EC/DEC electrolyte (1:1 volume-ratio mixture of ethylene carbonate and dimethyl carbonate, BASF, USA). The wire-shaped electrode was fabricated by coating electrode slurry on a 30 µm-diameter carbon wire (WPI, Sarasota, FL, USA). The slurry was composed of 50 wt% active material ($Ge_{0.9}Se_{0.1}$), 30 wt% conductive carbon (C65, TIMCAL) and 20 wt% carboxymethyl cellulose binder (Sigma-Aldrich, pre-dissolved in deionized water). The micrometer-sized $Ge_{0.9}Se_{0.1}$ particles were provided by C. B. Mullins's group (Klavetter *et al.*, 2015). The quartz capillary housing and carbon-wire current collector were selected because of their low X-ray attenuation. TXM tomography was implemented under an X-ray energy of 11.2 keV at the beamline 32-ID-C of the Advanced Photon Source (APS). The photon rate in a field of view of around 74.6 µm is approximately 1.17×10^{11} photons s^{-1} at 11.2 keV at this beamline. The illumination at the edges of the field is weaker, which results in lower radiation dose at the edges of the field of view. The wire electrode is located at the center of the field view and is about 39.1 µm × 60.1 µm in the projection image. The photon rate in this area is approximately 7.12×10^{10} photons s^{-1}, which is calculated from the intensity profile of a flat-view image. It should be noted that the radiation intensity is reduced by approximately 2.8% and 11.7% before reaching the wire electrode by the 10 µm-thick wall of quartz capillary and the 200 µm-thick electrolyte in the capillary, respectively. By comparing the intensity profiles of a flat-view image and an electrode image, the electrode absorbs approximately 1.2% of the photon intensity illuminated on it.

3. Results and discussion

To specify radiation damage under an *in situ* environment, the $Ge_{0.9}Se_{0.1}$ electrode was exposed to X-rays with a photon energy of 11.2 keV during ∼12 min of TXM tomography measurement. Seven hundred and twenty-one TXM images were captured for 1 s of X-ray exposure at 0.25° rotation increments over 180°. Fig. 1 shows TXM images at various rotation angles. The TXM images depict the $Ge_{0.9}Se_{0.1}$ particle cluster of the electrode in bright color with a pixel size of 37.7 nm (imaging resolution). Reconstruction of raw tomography data requires retaining the structure of the sample during 180° rotation. Thus, the initial (0°) and final (180°) TXM images should be symmetric to reconstruct the electrode microstructure. However, the final TXM image shows large changes of $Ge_{0.9}Se_{0.1}$ particle cluster after ∼12 min of X-ray exposure. Video S1 (see supporting information) clearly shows the following morphology changes of the electrode: (1) growing distances between particles, and (2) sudden particle dislocations (*e.g.* Δx and Δy in Fig. 1). The morphology changes are considered to be as a result of the radiation damage on the carbon–binder matrix of the irradiated electrode.

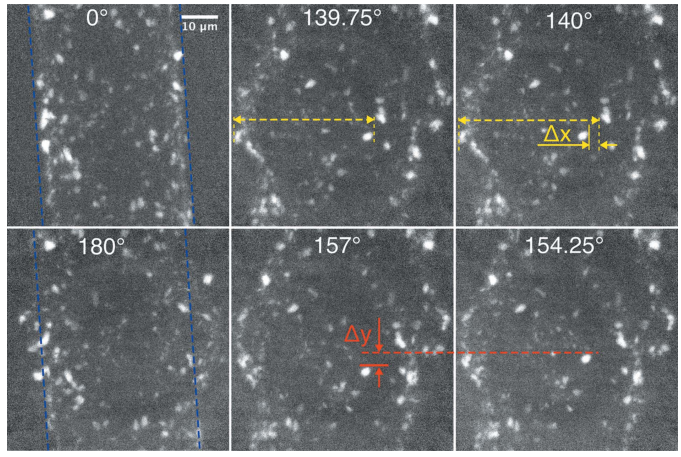

Figure 1
TXM images of a $Ge_{0.9}Se_{0.1}$ electrode in *in situ* experimental environment at different angles during tomography under 11.2 keV photon energy. The blue dashed lines at 0° and 180° show particle cluster changes after 12 min of irradiation. The 180° image was horizontally flipped to directly compare with the 0° image. Δx and Δy show sudden particle dislocation due to the change of the carbon–binder matrix.

To investigate the effect of radiation dose on the carbon–binder matrix, a $Ge_{0.9}Se_{0.1}$ electrode in electrolyte environment was exposed to 11.2 keV X-rays and monitored by continuously capturing TXM images with 1 s exposure for 30 min without sample rotation. Fig. 2(*a*) shows 1 s and 30 min irradiated $Ge_{0.9}Se_{0.1}$ clusters and Video S2 shows the dynamic change. The TXM images clearly show the change of particle clusters during 30 min of irradiation. To quantify the radiation damage, two of the particle distances [marked as L_1 and L_2 in Fig. 2(*a*)] were tracked by the irradiation time. In Fig. 2(*b*), the onset of distance increment (ΔL_1) appeared at 6 min and ΔL_1 reached 5.4% of the initial distance after 30 min of irradiation. The distance increment (ΔL_2) shows a similar pattern to ΔL_1, but its onset appeared at 4 min and is 9.4% of the initial distance after 30 min of irradiation. The faster and larger change of L_2 is due to the higher X-ray dose in the middle of the illumination field. To test whether the damage on the carbon–binder matrix is primarily from free radicals released from the absorption of photons by Ge, the same experiment was conducted at 11.2 keV (after Ge *K*-edge) and 11 keV (before Ge *K*-edge). As the $Ge_{0.9}Se_{0.1}$ particle size is about 2 µm, the X-ray absorption of $Ge_{0.9}Se_{0.1}$ particles at 11.2 keV is about six times the absorption at 11 keV. In order to only compare the impact of the energy level, two regions on one wire $Ge_{0.9}Se_{0.1}$ electrode with similar dimensions were selected. Fig. S1 and Videos S3 and S4 show that the expansion of the $Ge_{0.9}Se_{0.1}$ electrode at two energy levels is similar, which demonstrates that the damage is primarily from the absorption of photons by the carbon–binder matrix.

We believe that synchrotron X-ray radiation can have two effects on the polymer binder: scission and crosslinking (Coffey *et al.*, 2002). Scission of a long-chain polymer generates short-chain polymers, which could be dissolved by the electrolyte. Therefore, some $Ge_{0.9}Se_{0.1}$ particles could be suddenly dislocated from the particle cluster. Crosslinking of

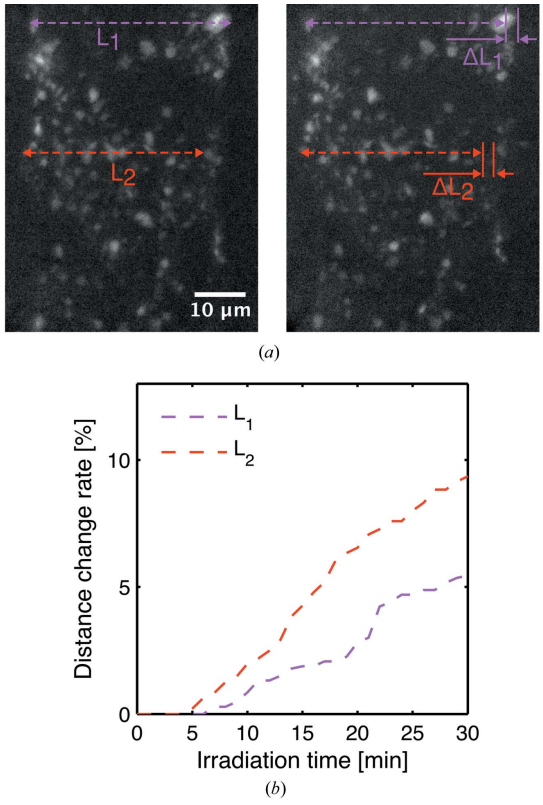

Figure 2
A series of TXM images with 1 s exposure are captured to monitor radiation damage on a $Ge_{0.9}Se_{0.1}$ electrode in electrolyte environment under 11.2 keV photon energy. The TXM images show (*a*) 1 s (left) and 30 min (right) irradiated $Ge_{0.9}Se_{0.1}$ particle cluster with 37.7 nm pixel resolution. (*b*) The increment of particle distances is tracked by the accumulated X-ray dose.

the polymer could cause swelling of the polymer in electrolyte, which is the reason for the expansion of the carbon–binder matrix. The distance tracking results indicate that the carbon–binder matrix maintains the $Ge_{0.9}Se_{0.1}$ particle cluster under the 11.2 keV X-rays for 4 min. Thus, the irradiation dose can be reduced to sustain the structure during TXM tomography. However, reducing the total dose means decreasing the number of images or the exposure time. Both will reduce the quality of tomography. Typically, tomography collects a series of TXM images under continuous X-ray exposure. For instance, the $Ge_{0.9}Se_{0.1}$ electrode has about 6 min of total X-ray exposure if 361 images with 1 s exposure and 180° rotation are used. The 6 min of continuous X-ray illumination can cause a change to the structure of the electrode by the damaged carbon–binder matrix. Vaselabadi *et al.* (2016) showed that radiation damage on polymers is likely to have an onset dose. If intermittent exposure was implemented with each exposure dose smaller than the onset dose and a long enough interval time between exposures, it is hypothesized that the radiation damage can be significantly reduced or avoided.

To test this hypothesis, X-rays were exposed for 1 s to capture an image and blocked by a shutter for 3–8 s before capturing the next image during *in situ* TXM tomography.

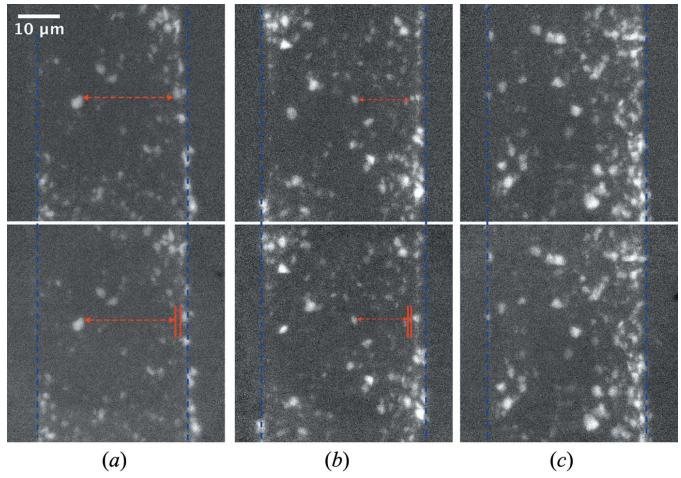

Figure 3
In situ TXM tomography of a $Ge_{0.9}Se_{0.1}$ electrode under intermittent 11.2 keV photon energy. TXM images show the $Ge_{0.9}Se_{0.1}$ particle cluster with a 37.7 nm-pixel resolution at the initial position (0°, top) and the horizontally flipped image at the last position (180°, bottom). The series of TXM images with 1 s exposure are obtained with (*a*) 3 s, (*b*) 5 s and (*c*) 8 s blocking time. The red marks indicate particle distance increments (*a*) 5.3% and (*b*) 2.6% after the TXM tomography.

Fig. 3 shows the initial and horizontally flipped last images of the TXM tomography with three different X-ray blocking times (3, 5 and 8 s). The dashed lines were drawn based on the initial TXM images to show the particle cluster changes after the tomography. The biggest increment of particle distance is around 5.3% with the 3 s blocking time shown in Fig. 3(*a*) and it is around 2.6% with the 5 s blocking time shown in Fig. 3(*b*). As shown in Fig. 3(*c*), the 8 s blocking time allows the particle cluster to be maintained during the *in situ* TXM tomography. The series of TXM images demonstrate the stable electrode structure during the tomography with 8 s blocking time in Video S5. The result suggests that radiation-induced morphology changes in *in situ* TXM tomography could be avoided by minimizing the accumulated X-ray dose and choosing intermittent X-ray exposure. It should be noted that radiation damage on the carbon–binder matrix could already start before the morphology change is detected at 4 min of continuous exposure. The undetected changes can de-activate some $Ge_{0.9}Se_{0.1}$ particles by breaking electronic connection. Radiation damage on the carbon–binder matrix depends on many factors, such as polymer materials, electrolyte, photon energy, photon rate, *etc*. The dose plan should be set based on the *in situ* experimental conditions. Another option to avoid the impact of radiation damage on the carbon–binder matrix is to use other binding techniques instead of a polymer binder. For instance, Wang *et al.* (2014) directly deposited Sn particles on a carbon substrate and conducted *in situ* TXM tomography successfully.

4. Conclusions

Radiation-induced damage of LIB electrodes was investigated in electrolyte environment for *in situ* TXM tomography.

Particle cluster changes of the irradiated electrode revealed radiation damage on the carbon–binder matrix. Irradiation of the carbon–binder matrix induces scission and crosslinking of the polymer, which causes the dislocation of active material particles and an expansion of the carbon–binder matrix. The radiation damage on the carbon–binder matrix during TXM tomography can be avoided by minimizing the total irradiation dose and choosing intermittent X-ray exposure.

Acknowledgements

This work used resources of the Advanced Photon Source, a US Department of Energy (DOE) Office of Science User Facility operated for the DOE Office of Science by Argonne National Laboratory under contract No. DE-AC02-06CH11357.

Funding information

Funding for this research was provided by: US National Science Foundation (award No. 1335850).

References

Coffey, T., Urquhart, S. & Ade, H. (2002). *J. Electron Spectrosc. Relat. Phenom.* **122**, 65–78.

Klavetter, K. C., Pedro de Souza, J., Heller, A. & Mullins, C. B. (2015). *J. Mater. Chem. A*, **3**, 5829–5834.

Lim, C., Yan, B., Kang, H., Song, Z., Lee, W. C., De Andrade, V., De Carlo, F., Yin, L., Kim, Y. & Zhu, L. (2016). *J. Power Sources*, **328**, 46–55.

Nelson, J., Yang, Y., Misra, S., Andrews, J. C., Cui, Y. & Toney, M. F. (2013). *Proc. SPIE*, **8851**, 88510B.

Vaselabadi, S. A., Shakarisaz, D., Ruchhoeft, P., Strzalka, J. & Stein, G. E. (2016). *J. Polym. Sci. B*, **54**, 1074–1086.

Wang, J., Chen-Wiegart, Y. K. & Wang, J. (2014). *Angew. Chem.* **126**, 4549–4553.

Weker, J. N., Liu, N., Misra, S., Andrews, J., Cui, Y. & Toney, M. (2014). *Energy Environ. Sci.* **7**, 2771–2777.